

Article

The SMILE Effect in the Beam Propagation Direction Affects the Beam Shaping of a Semiconductor Laser Bar Array

Hongyou Zhang ^{1,2,*} , Yu Hu ^{2,3} , Shuihai Peng ^{1,2} and Yong Liu ^{1,*}

¹ State Key Laboratory of Electronic Thin Films and Integrated Devices, School of Optoelectronic Science and Engineering, University of Electronic Science and Technology of China, Chengdu 610054, China; cathy.peng@xgimi.com

² XGIMI Technology Co., Ltd., Chengdu 610095, China; daniel.hu@xgimi.com

³ School of Life Science and Technology, University of Electronic Science and Technology of China, Chengdu 610054, China

* Correspondence: hongyou.zhang@xgimi.com (H.Z.); yongliu@uestc.edu.cn (Y.L.)

Abstract: Near-field bending of a laser diode bar (i.e., the SMILE effect) degrades the laser beam brightness, adversely affecting optical coupling and beam shaping. Previous reports mainly focused on the two-dimensional near-field bending of a laser diode bar. However, the near-field bending of a laser diode bar not only occurs in the laser bar growth direction, but also in the beam propagation direction. The present article proposes the three-dimensional near-field bending of a laser diode array, which is commonly known as the three-dimensional spatial SMILE effect. Through theoretical and simulated investigations, it has been found that a laser bar array not only deforms in the fast axis direction to cause the traditional two-dimensional SMILE effect but also experiences an additional deformation of approximately 2 μm in the laser emission direction simultaneously. Due to the SMILE effect in the beam propagation direction, not all emitters are aligned in a straight line, and some emitters experience defocusing during collimation. Consequently, there is an increase in the residual divergence angle and beam width, resulting in a degradation of the laser bar array's beam quality. According to the theoretical calculations, ZEMAX simulations, and experimental results, for a FAC (fast axis collimation) with a focal length of 300 μm , the divergence angle of single emitter after collimating in the fast axis increases from 4.95 mrad to 6.46 mrad when the offsetting of the working distance between the incident beam waist and FAC lens increases from 0 μm to 2 μm .



Citation: Zhang, H.; Hu, Y.; Peng, S.; Liu, Y. The SMILE Effect in the Beam Propagation Direction Affects the Beam Shaping of a Semiconductor Laser Bar Array. *Photonics* **2024**, *11*, 161. <https://doi.org/10.3390/photonics11020161>

Received: 7 November 2023

Revised: 2 February 2024

Accepted: 5 February 2024

Published: 7 February 2024



Copyright: © 2024 by the authors. Licensee MDPI, Basel, Switzerland. This article is an open access article distributed under the terms and conditions of the Creative Commons Attribution (CC BY) license (<https://creativecommons.org/licenses/by/4.0/>).

Keywords: SMILE effect; beam shaping; semiconductor laser

1. Introduction

The utilization of high-power laser diodes has found extensive applications across various fields, including industry, scientific research, military operations, and medical treatments. A high beam quality is necessary to meet the requirements for high-power laser diode array (LDA) pumping and materials processing in the industry application. However, during the cooling process from the solder melting point to room temperature when packaging a laser diode, mechanical stress is induced due to the inadequate coefficient of thermal expansion (CTE) between the chip (typical GaAs 6.5 ppm/K) and the heat sink (typically made of copper, with a CTE of 16.5 ppm/K in this study), resulting in chip deformation known as the “SMILE” effect. Numerous previous reports have extensively investigated various aspects of the SMILE effect. These studies have primarily focused on comprehending the underlying mechanism behind the SMILE effect, elucidating its intricate workings, and providing valuable insights into this phenomenon [1,2]. Furthermore, researchers have devoted their efforts to developing effective testing methodologies for evaluating the presence and magnitude of the SMILE effect [3–5]. Moreover, scientists have also explored diverse strategies to mitigate or reduce the impact of the SMILE effect. By investigating innovative techniques and approaches, they strive to minimize any adverse

consequences that are associated with this phenomenon [6–8]. It is also equally crucial to comprehend the impact of the SMILE effect on diverse applications [9]. In summary, previous studies on the SMILE effect have covered a wide range of topics, including investigating its underlying mechanism, developing testing methodologies, and exploring strategies to mitigate its impact. However, the previous reports mainly focused on the two-dimensional near-field bending of a laser diode array, meaning that the three-dimensional near-field bending of a laser diode array is blank, especially for the near-field bending of a laser diode array in the beam propagation direction. Forrer et al. [10] reported that FACET BENDING in the laser emission direction and its effect could be observed, but the analysis and discussion about the effect of FACET BENDING on the beam shaping quality were missing. The traditional two-dimensional SMILE effect is caused by the packaging-induced stress in the x -axis direction (slow axis direction), as shown in Figure 1. The tensile stress applied to the top of the heat sink reduces its shrinkage, resulting in slower shrinkage at the top compared to the bottom and causing deformation of the heat sink in the z -axis direction. Due to the fact that the tensile strength of the heat sink is greater than that of the laser bar, deformation occurs in the heat sink, resulting in the SMILE effect in the fast axis direction, as shown in Figure 2a.

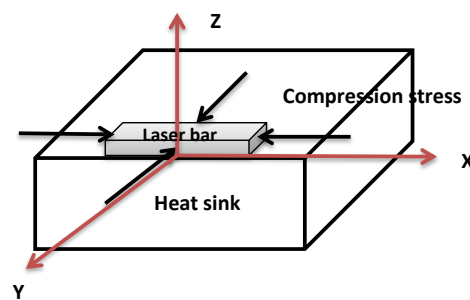


Figure 1. The force analysis diagram shows that the laser bar bonded on a heat sink experiences packaging-induced stress not only in the X -axis direction (slow axis direction) but also in the Y -axis direction (fast axis direction). The arrows indicate the direction of applied force.

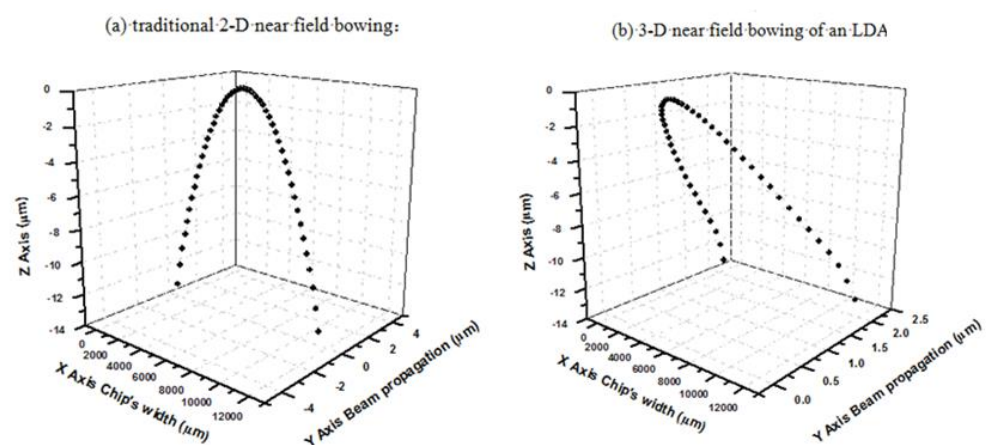


Figure 2. The simulation results of the near-field bending of a laser diode array are shown: (a) traditional two-dimensional near-field bending and (b) three-dimensional near-field bending of a laser diode array. Each black data point in the figures represents a single emitter of the laser diode array. In the three-dimensional near-field bending of a laser diode array, each emitter (black data point) is not only non-linear in the fast axis but also not aligned with the laser emission direction.

However, the tensile or compression stress that is applied to both the heat sink and laser bar is not only in the x -axis direction but also in the y -axis direction. The tensile stress that is applied to the front of the heat sink reduces its shrinkage, resulting in slower shrinkage on the front compared to the back side. This leads to deformation of the heat

sink in the y -axis direction and near-field bending of a laser diode array in the beam propagation direction. Combining the near-field bending in the z -axis direction and in the beam propagation (y -axis) direction, the near-field bending of a laser diode array should be three-dimensional spatially, as shown in Figure 2b.

The SMILE effect in the beam propagation direction was tested by using a surface profile measuring instrument (Veeco, Plainview, NY, USA), as shown in Figure 3. The SMILE value in the beam propagation direction was calculated by testing the surface profile of the laser diode array facet both before and after bonding. The device under test is a typical laser diode array, consisting of a cm bar (typically GaAs: 10 mm in width, 0.125 mm in height, and 2.0 mm in cavity length) that is securely bonded to a CuW submount (typically measuring 10.2 mm in width, 0.3 mm in height, and 2.25 mm in length), which is then affixed to a conductive cooling heat sink (typically made of copper alloy and measuring 10.6 mm in width, 7.65 mm in height, and 27 mm in length).

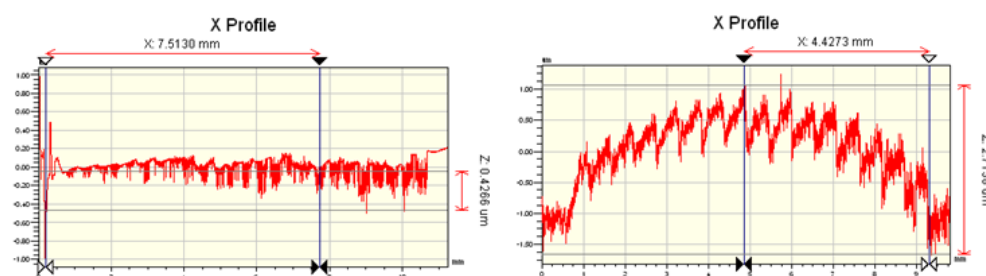


Figure 3. The SMILE value in the beam propagation direction is $0.4 \mu\text{m}$ before bonding (as shown on the (left)) and $2.7 \mu\text{m}$ after bonding (as shown on the (right)). The abscissa axis represents the width of the laser bar array (cm bar), while the vertical coordinate represents the deformation of the laser diode array facet (SMILE effect in the beam propagation direction).

The primary focus of this report is to investigate the three-dimensional near-field bending phenomenon in a laser diode array, specifically examining the SMILE effect in the beam propagation direction and its impact on beam shaping. Firstly, we propose a theoretical analysis of the three-dimensional spatial SMILE effect and near-field bending in the laser emission direction. Subsequently, we conduct theoretical calculations, simulations, and experiments to investigate the effects of near-field bending in the laser emission direction. After conducting a thorough comparison of theoretical calculations, ZEMAX simulations, and experimental results, we successfully validate our assertions regarding the three-dimensional spatial SMILE effect, particularly its impact on near-field bending in the direction of laser emission and beam shaping. Due to the SMILE effect in the beam propagation direction, not all emitters are perfectly aligned, and some experience defocusing during collimation. Consequently, there is an increase in the residual divergence angle and beam width, resulting in a deterioration of the laser bar array's beam quality. The findings of this research hold immense importance in the field of semiconductor laser beam shaping.

2. Theoretical Analysis

Three main factors affect the beam shaping quality in the fast axis, including the traditional SMILE effect in the fast axis direction [7], a bent FAC lens, and the SMILE effect in the laser emission direction. It has been reported that a $5 \mu\text{m}$ traditional SMILE value may reduce the beam quality by a factor of 2 [7]. It is well known that a bent FAC lens due to machining tolerance mismatch will cause a change in distance between the emitter and the FAC lens, thereby affecting the beam shaping quality. In this report, we will mainly discuss the effect of the SMILE value in the laser emission direction and its impact on the beam shaping quality. We assume that the traditional SMILE value remains unchanged, and there is no bending in the FAC lens for this study.

An individual FAC lens (FAC 300 from LIMO, Dortmund, Germany) is attached to a laser diode array during the manufacturing stage, where the FAC lens with a focal length 300 μm should be considered in its six degrees of freedom [11], $\Delta x, \Delta y, \Delta z$ represent the position error, and $\theta_x, \theta_y, \theta_z$ represent the angle error, as shown in Figure 4.

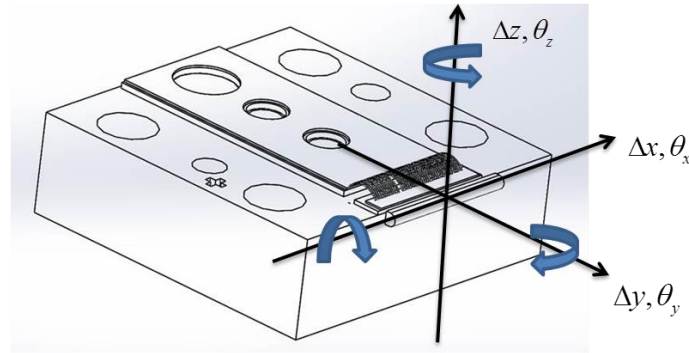


Figure 4. The schematic diagram shows an individual FAC 300 lens from LIMO being attached to a conductive cooling device, where the position errors $\Delta x, \Delta y,$ and Δz represent the positional error, and $\theta_x, \theta_y,$ and θ_z represent the angular errors of the FAC lens in its six degrees of freedom.

Achieving a high beam quality requires that each collimated emitter has to propagate in the same direction. The precise adjustment of the six degrees of freedom and achieving an optimal alignment of the FAC lens are crucial in order to prevent further degradation of the beam quality. The linear translation in the z-direction causes off-axial aberration, which is similar to the traditional two-dimensional SMILE effect in the fast axis direction, resulting in an increase in the divergence angle. The linear translation in the y-direction and tilt of θ_z will cause some emitters to be out of focus. By changing the axial position of an FAC lens in the y-direction, the beam of a laser diode array diverges uniformly, and the beam width increases. The tilt of θ_z around the central axis causes an axial displacement of the edges of the FAC, resulting in a divergence distribution that increases from a minimum at the center to a maximum along the edges of the laser diode array [11].

Figure 5 illustrates the geometry and provides more detail of the beam propagation path. In the fast axis, the laser beam should be a Gaussian beam. The Gaussian beam propagation path is studied by using the q parameter in this paper, as shown in Figure 5.

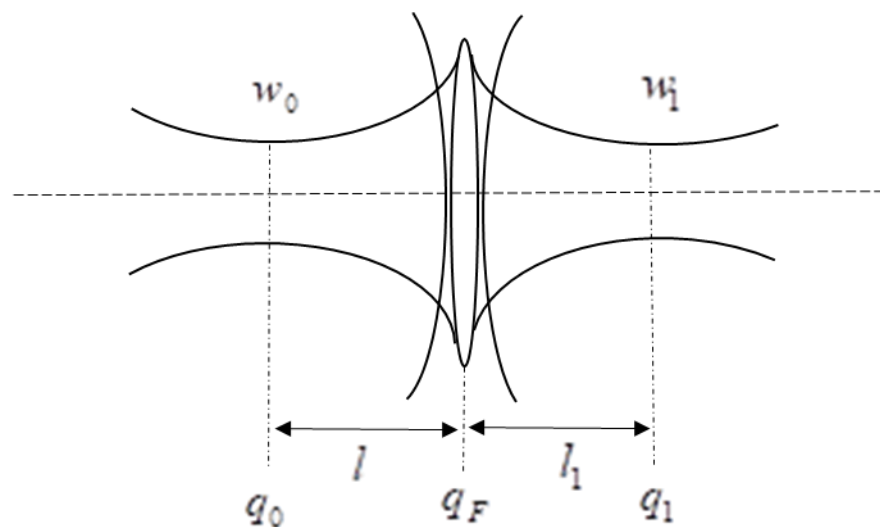


Figure 5. Schematic diagram illustrating the transmission of a Gaussian beam through a thin lens.

By utilizing the fundamental rule of the ABCD optical system [12] and q parameter, the beam waist's radius of the emergent light can be calculated.

$$\frac{1}{q(z)} = \frac{1}{R(z)} - i \frac{\lambda}{\pi w^2(z)} \tag{1}$$

where $R(z)$ represents the curvature radius of the incident wave front, and $w(z)$ represents the cross-section diameter of a Gaussian beam.

$$R(z) = z \left[1 + \left(\frac{\pi w_0^2}{\lambda z} \right)^2 \right], \quad w^2(z) = w_0^2 \left[1 + \left(\frac{\lambda z}{\pi w_0} \right)^2 \right] \tag{2}$$

Regarding Figure 5, q_0 represents the q parameter at the beam waist of the incident Gaussian beam, q_F represents the q parameter in the lens's exit plane, and q_1 represents the q parameter in the beam waist of the emergent Gaussian beam. Then,

$$q_0 = i \frac{\pi w_0^2}{\lambda} \tag{3}$$

$$q_F = q_1 - l_1 = i \frac{\pi w_1^2}{\lambda} - l_1 \tag{4}$$

Based on the fundamental rule of the ABCD optical system,

$$\begin{bmatrix} A & B \\ C & D \end{bmatrix} = \begin{bmatrix} 1 & 0 \\ -\frac{1}{F} & 1 \end{bmatrix} \begin{bmatrix} 1 & l \\ 0 & 1 \end{bmatrix} = \begin{bmatrix} 1 & l \\ -\frac{1}{F} & 1 - \frac{l}{F} \end{bmatrix} \tag{5}$$

Then,

$$q_F = \frac{Aq_0 + B}{Cq_0 + D} = \frac{i \frac{\pi w_0^2}{\lambda} + l}{-\frac{1}{F} i \frac{\pi w_0^2}{\lambda} + (1 - \frac{l}{F})} = i \frac{\pi w_1^2}{\lambda} - l_1 \tag{6}$$

The real and imaginary components in Equation (6) should be equal. The expression of the radius of the beam waist after the beam passes through the lens is

$$w_1^2 = \frac{F^2 w_0^2}{(F - l)^2 + \left(\frac{\pi w_0^2}{\lambda} \right)^2} \tag{7}$$

According to the relationship between the beam waist radius and the $1/e^2$ residual divergence angle of the Gaussian beam, λ represents the wavelength of emergent light. Then,

$$\theta_0 = 2 \frac{\lambda}{\pi w_0} \tag{8}$$

After collimating in the fast axis by using an FAC lens with a focal length of F , the residual divergence angle can be calculated.

$$\theta_1 = 2 \frac{\lambda}{\pi w_1} \tag{9}$$

According to Equation (8), the $1/e^2$ residual divergence angle will be

$$\theta_1 = \frac{2\lambda}{\pi} \sqrt{\frac{1}{w_0^2} \left(1 - \frac{l}{F} \right)^2 + \frac{1}{F^2} \left(\frac{\pi w_0}{\lambda} \right)^2} \tag{10}$$

The beam waist radius of the incident Gaussian beam is w_0 , and the distance between the incident beam waist and the FAC lens is l . The focal length of the FAC lens is F .

Regarding Equation (10), the residual divergence angle of the same laser diode array is influenced by both the focal length F of the FAC lens and the distance l between the incident beam waist and the FAC lens. The $1/e^2$ residual divergence angle changes in the same way as the function of F and l , as shown in Figure 6. The relationship between the working distance offset and the $1/e^2$ residual divergence of a single emitter angle after collimation with FAC 300 in the fast axis is calculated using the complex parameter representation of a Gaussian beam and the transformation formula of a thin lens.

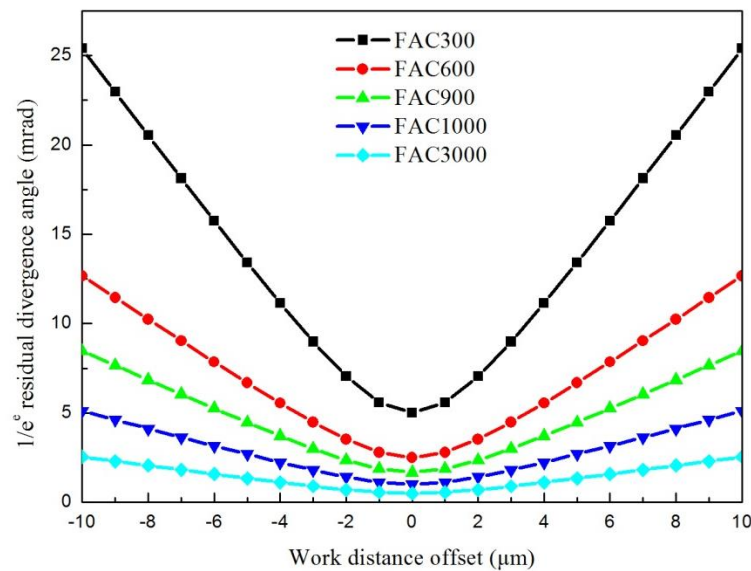


Figure 6. The $1/e^2$ residual divergence angle changes as a function of the focal length F of the FAC lens and the distance between the incident beam waist and FAC lens. FAC 300 refers to an FAC lens with a focal length of 300 μm .

In the theoretical calculation, we use a Gaussian beam through a thin lens model to express and calculate the beam transmission law for the purpose of facilitating the calculation. However, this paper utilizes non-spherical aspherical cylindrical lenses, which effectively address the high-order spherical aberration that is caused by a large aperture (NA) and are suitable for collimating semiconductor laser beams with a wide divergence angle in the fast axis direction. In this paper, we will focus on the effect of the three-dimensional spatial SMILE effect on the laser beam collimation. Therefore, our emphasis will be on analyzing the relative change in the collimation divergence angle resulting from variations in the beam propagation direction.

According to the theoretical calculation based on Equation (10) and Figure 6, the residual divergence angle is minimized when l is equal to the focal length of the FAC lens, and it increases whenever l is larger or smaller than the focal length of the FAC lens. Meanwhile, the residual divergence angle increases as the focal length of the FAC lens decreases.

The SMILE effect in the beam propagation direction produces the same results as the tilting of an FAC θ_z around its center axis does. When the emitter in the center is located at the focal point, the emitters along the edges of the laser diode array will be out of focus, resulting in a divergence distribution that increases from a minimum in the center to a maximum along the edges of the LDA. As shown in Figure 7, a curved laser bar where each emitter is not aligned in the laser emission direction causes some emitters to be placed out of focus. Due to the SMILE effect in the laser emission direction, there is a variation in the distance between the incident beam waist of each emitter and the FAC lens, resulting in nonuniform residual divergence angles for each emitter. When the distance l between the incident beam waist of a central emitter and the FAC lens is equal to the focal length of the FAC lens, the residual divergence of the central emitter is minimized. The distance

l_n between the emitter n and the FAC lens deviates maximally from the focal length of the FAC lens, resulting in the maximum residual divergence of emitter n in Figure 7. The difference value between l and l_n refers to the SMILE value in the laser emission direction.

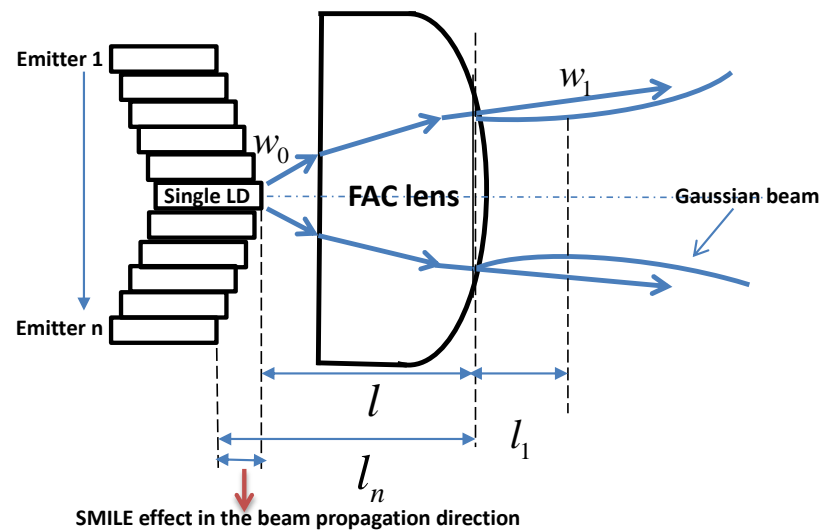


Figure 7. The near-field bending of a laser diode array in the beam propagation direction, as shown in the top view schematic diagram, affects the beam shaping of the laser diode array.

3. Simulation and Experiment

In the simulation, the residual divergence angle of two kinds of devices, including COC (chip-on-carrier) and CS (conductive cooling), are simulated after collimation in the fast axis. A single emitter (with a cavity length of 2 mm and a Fill Factor of 27%) is bonded onto a carrier to form a COC device emitting at a wavelength of 940 nm. The beam size before collimation is 1.5 μm in the fast axis and 135 μm in the slow axis. A laser bar with 19 emitters, which are the same as the emitter from COC, is bonded to a heat sink to form a CS device. An individual FAC lens (FAC 300 from LIMO) with a focal length of 300 μm is attached to a laser bar or a single emitter. We hypothesize that the traditional 2D SMILE value in the fast axis direction, as shown in Figure 1, remains unchanged and that there is zero bending of the FAC lens in the simulation. The Gaussian beam of a single emitter in the fast axis of a COC device is simulated using ZEMAX after collimating with FAC 300, as shown in Figure 8. The simulation involves varying the distance between the incident beam waist and the FAC lens to determine the beam width of the COC device after collimation. In the simulation, we utilize non-spherical aspheric cylindrical lenses, which effectively address the high-order spherical aberration that is caused by a large aperture (NA) and are suitable for collimating semiconductor laser beams with a wide divergence angle in the fast axis direction. The difference between the theoretical results of the Gaussian beam and ZEMAX calculations lies in the fact that ZEMAX software OpticStudio 20.1 is based on the geometric beam transmission principle for simulation, while the theoretical calculation is based on Gaussian beam transmission theory for analysis. The laser emitted from the fast axis direction of the semiconductor laser belongs to the fundamental-mode Gaussian beam. The ray tracing simulation software ZEMAX is used to analyze the geometric optical approximation, which may result in discrepancies between the simulation results and real-world situations.

According to the simulation results, the $1/e^2$ residual divergence angle of a COC device is 4.98 mrad, 5.1 mrad, 6.4 mrad, 7.8 mrad, 9.1 mrad, and 10.9 mrad when the working distance that is offset is 0 μm , 1 μm , 2 μm , 3 μm , 4 μm , and 5 μm . The beam width at a distance of 100 mm and $1/e^2$ residual divergence angle of a COC device changes as the function of the distance between the incident beam waist and the FAC lens, as shown in Figure 9. The beam width at a distance of 100 mm and the residual divergence angle

are minimized when the working distance is equal to the focal length of the FAC lens, and increase whenever the working distance is larger or smaller than the focal length of the FAC lens, which is in very good agreement with our theoretical calculation. The SMILE effect in the laser emission direction is caused by a change in the working distance that is offset between the laser diode and the FAC lens. By adjusting this offset, different values of the SMILE effect can be achieved and studied.



Figure 8. The Gaussian beam of a single emitter in the fast axis direction of a COC device is simulated using ZEMAX after collimating with FAC 300.

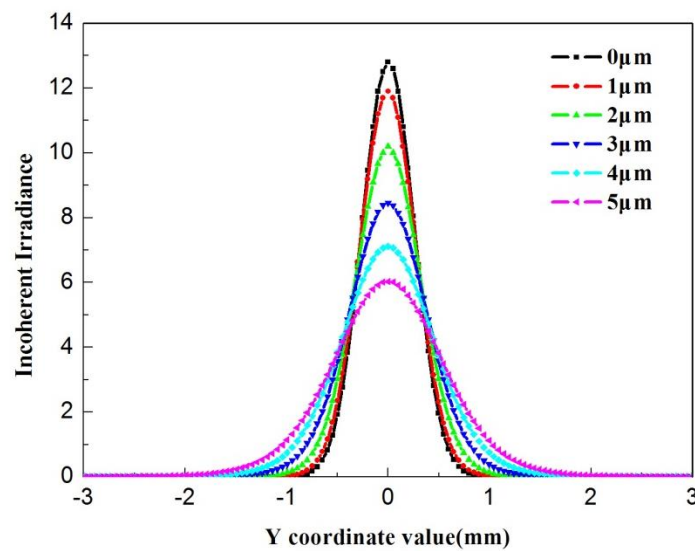


Figure 9. The Gaussian beam of a single emitter changes in the fast axis direction after collimating with FAC300 when the working distance that is offset increases from 0 μm to 5 μm.

The simulation results show that the residual divergence angle and beam width of a laser bar change as a function of the offsetting in the working distance. The distance between the incident beam waist of each emitter and the FAC lens is different due to the SMILE effect in the laser emission direction, resulting in nonuniformity in the residual divergence angle and beam width of each emitter, as shown in Figure 10. These findings are consistent with our theoretical analysis, as demonstrated in Figure 7.

According to the simulation results, axial defocusing causes the beam width to broaden and the residual divergence angle to increase. In the experiment, a COC device after collimation with the same parameters as in the simulation is tested for the beam width at a distance of 100 mm and $1/e^2$ residual divergence angle at different working distance offsets. Four COS devices after collimation with FAC 300 were tested for their beam width at different working distance offset, ranging from $-5 \mu\text{m}$ to $5 \mu\text{m}$. Figure 11b shows the testing results of one device, and all the testing results for beam width changes as a function of working distance offset are shown in Figure 11a.

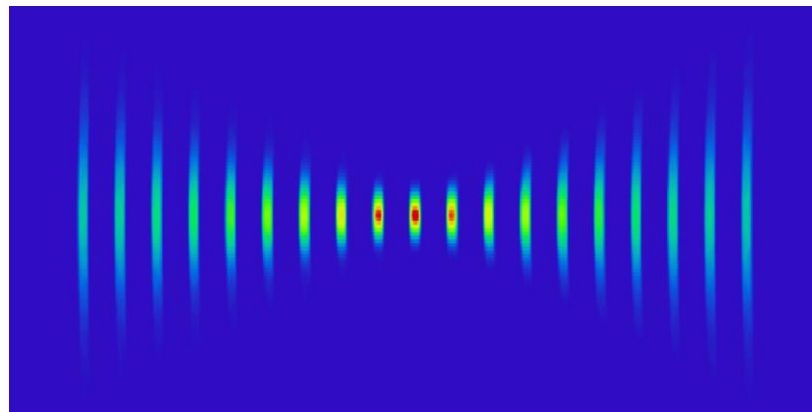


Figure 10. Beam shape of each emitter after FAC 300 collimating in fast axis direction, when assuming that the divergence angle is zero in the slow axis.

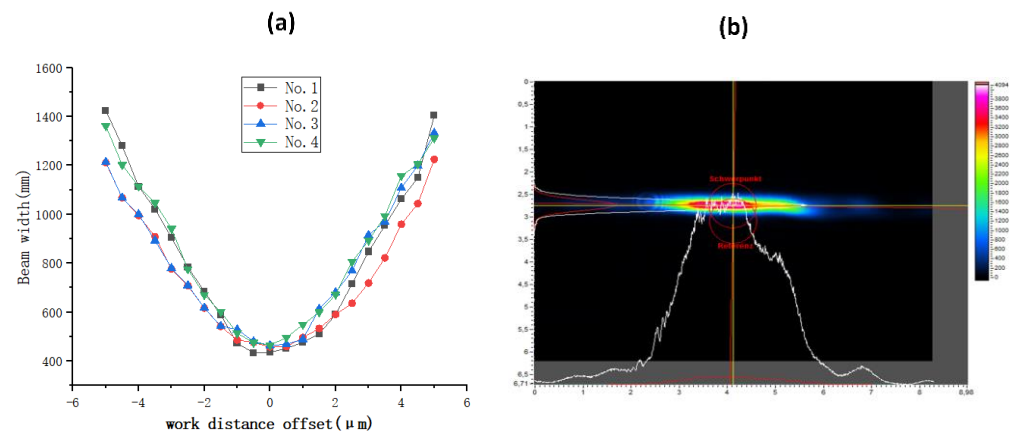


Figure 11. (a) The testing results for beam width changes as a function of working distance offset. (b) The testing results of one COS device.

The experimental results demonstrate a strong correlation with our theoretical calculations and simulation results, as depicted in Figure 12. The disparity between the experiment and theoretical calculation primarily arises from measurement errors and other factors, such as the two-dimensional traditional SMILE effect. Another possible reason is that the theoretical calculation uses the thin lens model, which assumes an ideal lens.

According to the theoretical calculation, ZEMAX simulation, and experimental results, the $1/e^2$ residual divergence angle of single emitter changes as the function of the working distance offset. The $1/e^2$ residual divergence of single emitter angle after collimation with FAC 300 in the fast axis direction increases from 4.95 mrad to 6.46 mrad when the working distance offset between the incident beam waist and the FAC lens increases from 0 μm to 2 μm . As mentioned before, the SMILE effect on the laser emission direction is caused by changing the working distance offset between the laser diode and the FAC lens. By adjusting the working distance offset, different values of SMILE effect on the laser emission direction can be achieved and studied. A 2 μm SMILE value in the laser emission direction causes an increase in the working distance offset between the laser diode and FACs to 2 μm . Due to the near-field bending of a laser diode array in the beam propagation direction, each emitter is not aligned in a straight line in the laser emission direction. As long as the center emitter is located at the focal point, parts of emitters are out of focus, resulting in a residual divergence angle distribution and increasing beam width from a minimum at the center to a maximum along the edges of the laser diode array. This leads to decreased beam quality.

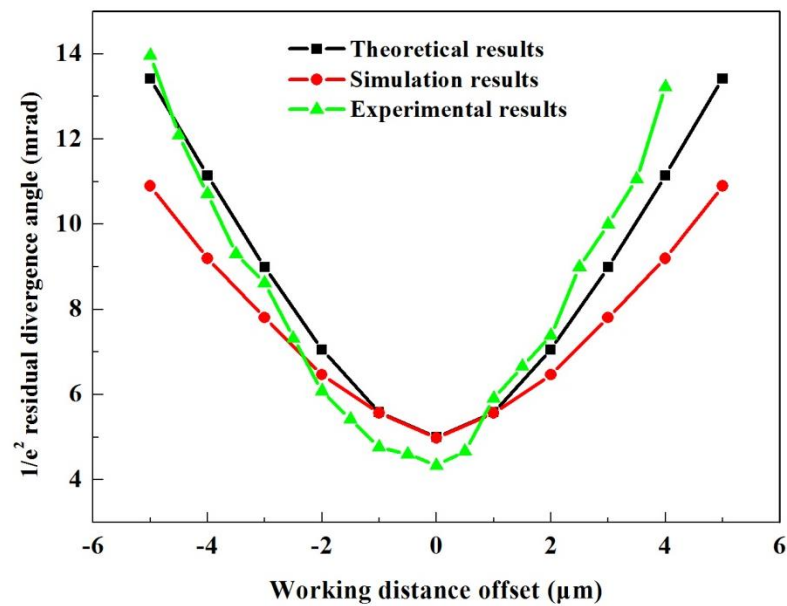


Figure 12. Theoretical calculation, ZEMAX simulation, and experimental results showing that $1/e^2$ residual divergence angle changes as a function of working distance offset.

The difference between the theoretical results of the Gaussian beam and ZEMAX calculations lies in the fact that the ZEMAX software OpticStudio 20.1 is based on the geometric beam transmission principle for simulation, while the theoretical calculation is based on Gaussian beam transmission theory for analysis. The laser that is emitted from the fast axis direction of the semiconductor laser belongs to the fundamental-mode Gaussian beam. The ray-tracing simulation ZEMAX software OpticStudio 20.1 is used to analyze the geometric optical approximation, which may result in discrepancies between the simulation results and real-world situations. Another possible reason is that the theoretical calculation uses the thin lens model, which assumes an ideal lens, while the simulation employs an aspherical lens, as shown in Figure 12. It has been found that the theoretical calculation results from Gaussian beam transmission transformation theory are closer to experimental results, indicating that using Gaussian transmission transformation theory can theoretically provide more accurate guidance for collimation experiments with single emitter semiconductor lasers. The advantage of ZEMAX software OpticStudio 20.1 simulation is that it can design and simulate multiple optical paths. Additionally, it can directly display the morphology and energy distribution of light spots, which is conducive to simulating the position of each lens and the direction of the optical path in experiments.

4. Conclusions

This article proposes the three-dimensional near-field bending of a laser diode array, referred to as the three-dimensional spatial SMILE effect. Unlike the traditional two-dimensional near-field bending of a laser diode array in the fast axis direction, the three-dimensional spatial SMILE effect demonstrates that a laser bar not only deforms in the fast axis direction to cause the traditional two-dimensional SMILE effect but also experiences approximately $2\ \mu\text{m}$ to $3\ \mu\text{m}$ deformation in the beam propagation direction simultaneously. The residual divergence angle varies as a function of the offset in working distance, as indicated by theoretical calculations, simulations, and experimental findings. A curved laser bar, with each emitter not being aligned in the direction of laser emission, causes some emitters to be placed out of focus. Due to the SMILE effect in the laser emission direction, there is a variation in the distance between the incident beam waist of each emitter and the FAC lens, resulting in nonuniform residual divergence angles for the individual emitter. If the emitter positioned at the center serves as the focal point, the emitters that are located along the periphery of the laser diode array will experience defocusing, leading to

a divergent distribution that progressively increases from a minimum value at the center to a maximum value towards the edges of the laser diode array.

According to the theoretical calculation, ZEMAX simulation, and experimental results, the $1/e^2$ residual divergence of single emitter angle after FAC 300 collimation in the fast axis direction increases from 4.95 mrad to 6.46 mrad when the working distance between the incident beam waist and the FAC lens increases from 0 μm to 2 μm . A 2 μm SMILE value in the laser emission direction causes an increase in the working distance offset between the laser diode and FACs to 2 μm . The effect of the SMILE value on the residual divergence decreases as the FAC focal length increases. The tolerance in the light propagation direction is 10 times higher for the FAC 3000 lens compared to the FAC 300 lens.

Author Contributions: Conceptualization, H.Z., Y.H., S.P. and Y.L.; methodology, H.Z. and Y.H.; software, S.P.; validation, H.Z. and S.P.; formal analysis, H.Z.; investigation, Y.H.; resources, H.Z.; data curation, H.Z.; writing—original draft preparation, H.Z.; writing—review and editing, H.Z. and Y.L.; visualization, H.Z.; supervision, Y.L.; project administration, H.Z.; funding acquisition, H.Z. and Y.L. All authors have read and agreed to the published version of the manuscript.

Funding: This research was found by the Project of Science and Technology of Sichuan Province (No. 2020YFG0453) and the Project of Science and Technology of Chengdu (No. 2020YFG0279) and (No. 2021YGC02).

Institutional Review Board Statement: Not applicable.

Informed Consent Statement: Not applicable.

Data Availability Statement: Data are contained within the article.

Conflicts of Interest: There is no conflict of interest between any of the authors and the company XGIMI Technology Co., Ltd.

References

1. Pao, Y.H.; Eisele, E. Interfacial shear and peel stresses in multilayered thin stacks subjected to uniform thermal loading. *J. Electron. Packag.* **1991**, *113*, 164–172. [[CrossRef](#)]
2. Wang, J.; Yuan, Z.; Kang, L.; Yang, K.; Zhang, Y.; Liu, X. Study of the mechanism of “smile” in high power diode laser arrays and strategies in improving near-field linearity. In Proceedings of the 2009 59th Electronic Components and Technology Conference, San Diego, CA, USA, 26–29 May 2009; IEEE: New York, NY, USA, 2009; pp. 837–842.
3. Herzog, W.D.; Ünlü, M.S.; Goldberg, B.B.; Rhodes, G.H.; Harder, C. Beam divergence and waist measurements of laser diodes by near-field scanning optical microscopy. *Appl. Phys. Lett.* **1997**, *70*, 688–690. [[CrossRef](#)]
4. Martí-López, L.; Ramos-de-Campos, J.A.; Martínez-Celorio, R.A. Interferometric method for characterizing the smile of laser diode bars. *Opt. Commun.* **2007**, *275*, 359–371. [[CrossRef](#)]
5. Martí-López, L.; Ramos-de-Campos, J.A.; Furlan, W.D. Analysis of the imaging method for assessment of the smile of laser diode bars. *Appl. Opt.* **2009**, *48*, 4880–4884. [[CrossRef](#)]
6. Zhang, H.; Chen, T.; Zhang, P.; Zah, C.E.; Liu, X. Effect of submount thickness on near-field bowing of laser diode arrays. *Appl. Opt.* **2018**, *57*, 8407–8411. [[CrossRef](#)] [[PubMed](#)]
7. Wetter, N.U. Three-fold effective brightness increase of laser diode bar emission by assessment and correction of diode array curvature. *Opt. Laser Technol.* **2001**, *33*, 181–187. [[CrossRef](#)]
8. Monjardin, J.F.; Nowak, K.M.; Baker, H.J.; Hall, D.R. Correction of beam errors in high power laser diode bars and stacks. *Opt. Express* **2006**, *14*, 8178–8183. [[CrossRef](#)] [[PubMed](#)]
9. Zhouping, S.; Qihong, L.; Jingxing, D.; Jun, Z.; Runrong, W. Beam quality improvement of laser diode array by using off-axis external cavity. *Opt. Express* **2007**, *15*, 11776–11780. [[CrossRef](#)] [[PubMed](#)]
10. Forrer, M.; Kura, D.; Langenbach, E. Micro-optic solutions for beam shaping of individually addressable high-power single-mode diode laser arrays. In *High-Power Diode Laser Technology and Applications VIII*; International Society for Optics and Photonics: Bellingham, WA, USA, 2010; Volume 7583, p. 75830D.
11. Bachmann, F.; Loosen, P.; Poprawe, R. (Eds.) *High Power Diode Lasers: Technology and Applications*; Springer: Berlin/Heidelberg, Germany, 2007; Volume 128.
12. Bélanger, P.A. Beam propagation and the ABCD ray matrices. *Opt. Lett.* **1991**, *16*, 196–198. [[CrossRef](#)] [[PubMed](#)]

Disclaimer/Publisher’s Note: The statements, opinions and data contained in all publications are solely those of the individual author(s) and contributor(s) and not of MDPI and/or the editor(s). MDPI and/or the editor(s) disclaim responsibility for any injury to people or property resulting from any ideas, methods, instructions or products referred to in the content.